Single Digit Region of Interest (SDROI) Extraction by Reducing the Tissue Influence

Dong Hua **Abdou Youssef**

Department of Computer Science, The George Washington University
801 22nd St. NW, Washington, DC 20052, USA
Email: gwuhua@gwu.edu, ayoussef@gwu.edu

Abstract

Hand X-ray images are often used for measuring skeleton developmental status via bone age assessment especially in children and adolescents. It forms an evidence for diagnostic use and treatment for various diseases such as metabolic and growth abnormalities. Traditional methods include the atlas matching by Greulich and Pyle (1971) and Tanner and Whitehouse (TW2). The general impression-based atlas matching often leads to error due to subjectivity while the high complexity of TW2 limits its use to within twenty percent. Efforts have been made intensively to computerize the entire process of bone age assessment to achieve both reliability and efficiency. One significant step towards this goal is to correctly extract the region of interest (ROI), which is usually small (e.g., knuckle). However, the non-uniformity of gray distribution, noise and angled posture of hand, often make the extraction of the ROI quite complicated. One possible solution is to extract a relatively large ROI within which those small particular ROIs are further investigated. By doing so, the influences of the above-stated factors are tackled by step-by-step 'zoom-in' and hence achieve extraction of small ROIs effectively. Unfortunately, the existence of tissue, especially on the metacarpals, often results in the ineffectiveness of various techniques (e.g., edge detection). In this paper, we develop an approach to solve this issue by using spectrum analysis as well as other image processing techniques. The effectiveness is shown by experiments on single-digit-region-of-interest (SDROI) extraction. 97% accuracy is achieved on one real data set.

1 Introduction

A common use of X-ray is to examine the patient's hand, either left or right, such that the produced images form an evidence for diagnosis and treatment of diseases in practice. These images are called hand X-ray images. Rich information contained in them, especially indicated by the ossifications centers (e.g., epiphysis), have been found helpful in assessment of bone age, a procedure for measuring the skeleton developmental status, especially in children and adolescents [1, 2, 10, 12, 20, 22]. Usually, the more inconsistency between bone age and chronological age implies the high abnormalities in skeletal development, which are associated with various behind diseases including endocrine disorders [4], metabolic and growth abnormalities [3], malformations and bone dysplasias [7], and gonadal dysgenesis [11], etc.

There are two conventional ways to achieve bone age assessment: one is the atlas matching by Greulich and Pyle (1971) [22]; and the other is Tanner and Whitehouse (TW2) (1975) [13] in the name of authors. The atlas matching is general impression-based, i.e., according to the human's decision on the entire image, leading to subjectivity and arbitrariness. In contrast, TW2 employs the strategy of 'distributed computing', that is, score individual bones in details and summarize them in the end. Such a method need special training for practicians and involves high complexity, which results in limited usage to be within twenty percent [10, 12].

Efforts have been made intensively to computerize the entire process of bone age assessment to achieve both reliability and efficiency. One significant step towards this goal is to extract the region of interest (ROI) (e.g., knuckle) and then describe them in terms of features for further use like classification for instance. Previous work includes Michael and Nelson (1989) [6], Levitt and Hedgcock (1989) [21], Pietka et al. (1991) [9], Wastl and Dickhaus (1996) [19], and Pietka et al. (2001) [8], etc. Specifically, Michael and Nelson (1989) [6] proposed a model-based computer vision system where the specific phalanges are segmented and measured in terms of several parameters (e.g., perimeter). Levitt and Hedgcock (1989) [21] applied the Bayesian inference technique to extract edges, regions, etc. where a structure of the hand is employed to identify the transverse edge and phalanx joints. In 1991, Pietka, McNitt-Gray and Huang [9] suggested the limitation in above two approaches and proposed a line scanning approach. Given a hand X-ray image, the phalangeal region of interest is defined and thresholded, and then the tip of third digit is located and a predefined window is shifted over the entire finger for length measurement of distal, middle, and proximal phalanx. Wastl and Dickhaus (1996) [19] used a semi-automatic segmentation method to locate region of interest in the phalangeal region as well as the wrist part. Such a method need pre-prepared markers on the image. A grid pattern approach was proposed by Pietka et al. (2001) [8] for extraction of phalangeal tip and then continue to extract epiphyseal/metaphyseal ROI (EMROI) for analysis. However, the ROI used is usually small, a specific knuckle for example. The non-uniformity of gray distribution, noise and angled posture of hand, often make the extraction of the ROI quite complicated. One possible solution is to extract a relatively large ROI, single digit region of interest (SDROI) for instance, within which those small particular ROIs are further investigated. By doing so, the influence of the above-stated factors are tackled by step-by-step 'zoom-in' and hence achieve extraction of small ROIs effectively. Unfortunately, the existence of tissue, especially on the metacarpals, often results in the ineffectiveness of various techniques (e.g., edge detection). Work of this paper is to deal with this issue aiming at improving the performance of SDROI extraction. Spectrum analysis as well as other image processing techniques are used. Effectiveness of the approach is shown by the experiment on one real data set, where the accuracy can reach 97% with using our approach to reduce the tissue influence while 86% is obtained if *not*.

1.1 Organization

The rest of this paper is organized as follows. In section 2, we introduce the method to handle the tissue influence for SDROI extraction. Experimental results on one real data set are shown in section 3 where evaluation and discussion of the performance are presented. Finally, section 4 provides the conclusion.

2 Method

In this section, the method to deal with tissue influence is given in order to improve the performance of SDROI extraction. Spectrum analysis and several other image processing techniques are used.

Given a hand X-ray image **I**, as shown in Fig. 1, the gray information can be represented by a matrix $\mathbf{G} = [X_{ij}]$ where $i = 1, \cdots, m$; $j = 1, \cdots, n$ and X_{ij} denotes the gray value of the pixel in the position of i_{th} row and j_{th} column. If we treat each column as a vector, then the spectrum along the columns is defined by:

$$\mathcal{P}_c = (\sum_i X_{i1}, \sum_i X_{i2}, \cdots, \sum_i X_{in}) / \sum_i X_{ik^*} \quad (1)$$

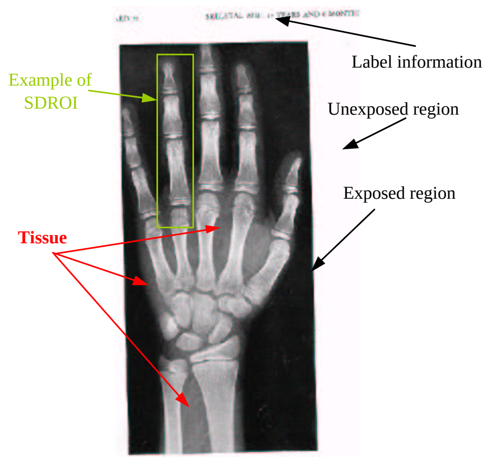

Figure 1: A source hand X-ray image.

where $k^* = arg\ \max_k\{\sum_i X_{ik}\}$. For the spectrum along rows, just flip the subscript and obtain:

$$\mathcal{P}_r = (\sum_j X_{1j}, \sum_j X_{2j}, \cdots, \sum_j X_{mj}) / \sum_j X_{l^*j} \quad (2)$$

where $l^* = arg\ \max_l\{\sum_j X_{lj}\}$. The spectrum is also defined in the same way for sub-matrix of **G**, i.e., sub-graph of **I**. The output spectrums, either or both of row and column spectrums, form the evidence for region detection and extraction by using other image processing techniques. These regions include unexposed region, phalangeal region, and single digit region, etc.

The entire process of the approach developed in this paper is performed through two stages, stage I: tissue region removing; and stage II: SDROI extraction for evaluation. Fig. 1 shows the tissue, indicated by red arrows, which attaches the bones with relatively low gray value. A typical SDROI contains a finger within phalangeal region of interest (PROI) as indicated by the example shown in Fig. 1, where the corresponding distal, middle, proximal phalanx and upper part of metacarpal as well as epiphyses and metaphyses among them are encapsulated.

2.1 Tissue region removing

Tissue is characterized by the regions with relatively low gray value, existing in appearance of attachment to bones. Actually, if we look from the opposite angle of view, bones are overwhelmed in tissue, especially the palm and wrist part. As such, all the tissue regions are connected to each other which can be treated as an entire structure. In particular, this structure cuts in the bottom edge of the image, with individual bones distributing among them. This observation motivated the strategy of 'image clear border' to remove tissue in this paper, that is, suppresses tissue structure that is lighter than its surroundings and that is connected to the image border. The function 'imclearborder' of Matlab is used in our implementation. This algorithm uses morphological reconstruction where input source images is the mask image and the marker image is zero everywhere except along the border, where it equals the mask image [17]. As cautioned by the manual of Matlab, for intensity images, 'imclearborder' tends to reduce the overall intensity level in addition to suppressing border structures. To achieve tissue removing, the resulting image after 'imclearborder' is thresholded further. The threshold is obtained by Otsu's method [16], which intends to minimize the intraclass variance of the thresholded black and white pixels. Specifically, we first detect the unexposed region by analyzing the spectrum of the image (see Fig. 2). After separating out the exposed region, we enforce the top, left, and right border to be black and the bottom border white in case of the undesired effect of 'imclearborder' on other regions.

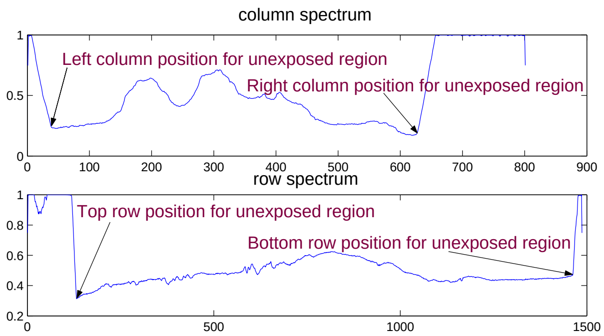

Figure 2: Spectrum for detecting the unexposed region.

2.2 SDROI extraction for evaluation

To extract SDROI, the spectrum-based method [5] is used. That is, we first extract the part of phalangeal region of interest (PROI) which contains phalanges, epiphyses, and upper part of metacarpals. This task is achieved by analyzing the row spectrum of the threshold image with no tissue removing. Usually, the peak value is the position where the PROI can be separated from the the rest part, namely, the most part of metacarpals, carpals, and upper part of the ulna and radius. Due to various factors (e.g., noise), such a peak value sometimes is not obvious. Hence, we often threshold the row spectrum and get a bunch of maxima $(p_1, p_2, \cdots, p_n)$. The final position for cutting the PROI is obtained using the median of these values, i.e., $p_{n/2}$ if n is even and $round((p_{(n-1)/2} + p_{(n+1)/2})/2)$ otherwise. This position is applied to the threshold image produced by stage I and the threshold PROI with tissue removing, $\mathbf{G_p}$, is obtained. Next is the rotation calibration. This is achieved by maximizing the variance of the column spectrum of $\mathbf{G_p}$ with at most ten times of rotation (e.g., 2 degree per time, either clockwise or counter clock-wise). Given a column spectrum $\mathcal{P}_c = (\sum_i X_{i1}, \sum_i X_{i2}, \cdots, \sum_i X_{in}) / \sum_i X_{ik^*}$ where $k^* = arg\ \max_k \{\sum_i X_{ik}\}$, the variance (bias-corrected sample variance) is $s^2_{N-1} = \frac{1}{N-1}\sum_{j=1}^{N}(\mathbf{x_j} - \bar{\mathbf{x}})$, where $\mathbf{x_j} = \sum_i X_{ij} / \sum_i X_{ik^*}$ and $\bar{\mathbf{x}} = \frac{1}{N}\sum_{j=1}^{N}\mathbf{x_j}$. After that, we threshold the column spectrum and find the positions of SDROIs. The corresponding threshold value is called SDROI threshold. Usually, different SDROI threshold values differ in the number of successfully extracted SDROIs due to noise, angled posture of fingers and non-consistency in their lengths, which will be seen in our experiments. Finally, these positions as well as the rotation degree are applied to the image after removing unexposed region. Individual SDROIs are hence obtained. In this paper, only the second, third, fourth and fifth digits are considered because the angled posture of the first digit makes its spectrum often unrecognized.

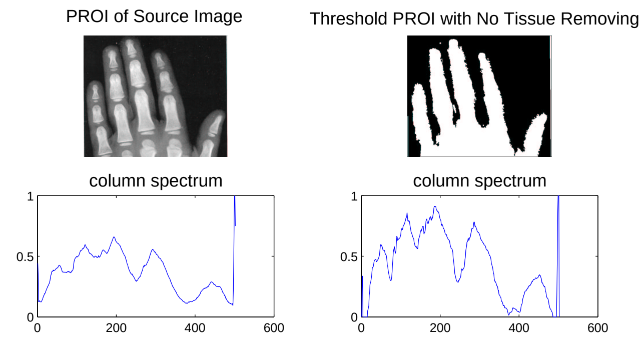

Figure 3: Example of spectrum analysis without reducing tissue influence.

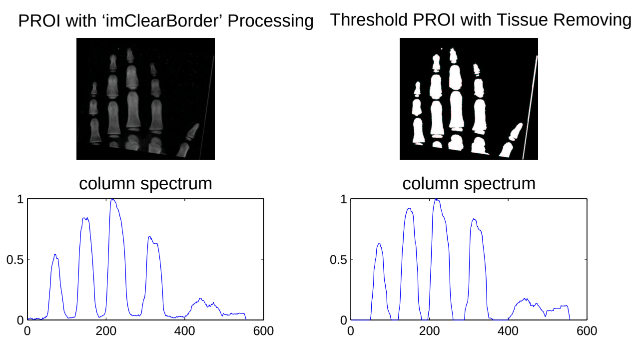

Figure 4: Example of spectrum analysis with reducing tissue influence.

As we mentioned before, the existence of tissue often results in ineffectiveness of various techniques, leading to the extraction of SDROI quite complicated for instance. Fig. 3 shows the effect of column spectrum if tissue is not removing, while Fig. 4 shows the effect with tissue removing, which is very friendly for detection of SDROIs' positions. In this case, we also find that the existence of tissue caused the rotation calibration unsuccessfully as implied by the images in Fig. 3. That is why tissue removing could improve the performance of SDROI extraction. Another reason is that the removing of tissue renders the digits appearing separated, which makes the spectrum distributed clearly with respect to the corresponding SDROIs.

3 Experimental Results

In this section, the effect of tissue removing is investigated over one real data set which is about children boys. It consists of 23 source hand X-ray images taken from the study on the skeleton development of children at different levels of bone age ranging from new born until 19 years old. Each image represents the typical skeleton developmental status of the entire hand w.r.t. the corresponding bone age.

Performance is evaluated in terms of the number of correctly extracted SDROIs for each source image and overall success rate w.r.t. each SDROI threshold value (see stage II of section 2). The SDROI threshold varies from 0.1 to 1.0 with step length 0.05. As such, nearly four hundred and fifty data points are available: 23×19 in total. Additionally, only four SDROIs, namely, the second, third, fourth and fifth SDROIs, for each hand X-ray image are investigated for reasons discussed previously. Therefore, the maximum of correctly extracted SDROIs is *four* and the minimum *zero*. Comparison of the results with tissue removing and *not* is given.

Table 2 summarizes the experiment result with tissue removing, while Table 1 *not*. The first row represents the corresponding value of SDROI threshold, the first column corresponds to the label information of each source hand X-ray image, and the rest data points denote the number of correctly extracted SDROIs in the scenario of all combinations of SDROI threshold and source images. The maximum number *four* is shaded. It is easy to see that the shaded area of Table 2 is larger than that of Table 1 indicating improved performance. If we count the number of data points which reach the maximum *four*, there are 104 in total for Table 1 while 168 for Table 2, improving about 61.5%. As for overall success rate, the best result achieved with no tissue removing, if the bad case 'MS4y6m' (digits overlap too much) is considered, is 86%, while with tissue removing the success rate could reach 92%. Without considering the case 'MS4y6m', the best result is 97% with tissue removing as compared 88% if *not*. Fig. 5 illustrates the comparison the overall success rate graphically showing the effectiveness of tissue removing on SDROI extraction.

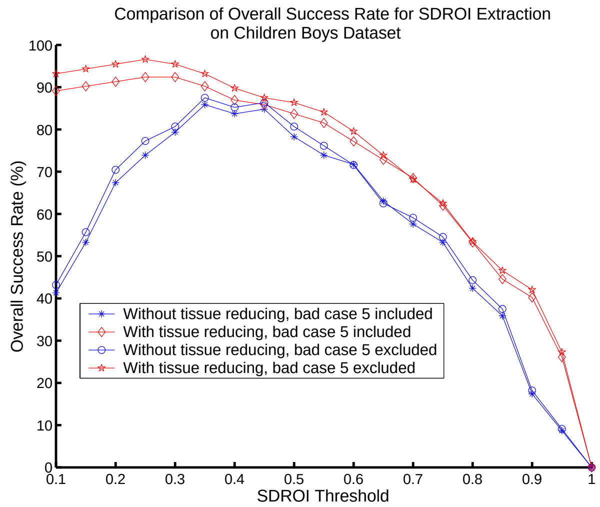

Figure 5: Comparison of Overall Success Rate for SDROI Extraction on Children Boys Dataset.

4 Conclusion

The task to computerize the entire process of bone age assessment is a significant step towards the goal of achieving both reliability and efficiency. Hand X-ray images are usually used for its benefits including convenience, health-care with least unexposed part of body under X-ray and rich ossification centers. Given a source image, a typical computerized approach is to extract region of interest (ROI) and then describe them in terms of features for further use. These ROIs are usually very small (e.g., epiphysis) which make straightforward extraction quite complicated due to the non-uniformity of gray distribution, noise and other kind of factors. Additionally, overwhelmed non-useful information v.s. the target small ROI even adds the difficulty. The single digit region of interest (SDROI) extraction is a possible solution, aiming at improving the small ROI extraction via first extracting the relatively large ROIs before further small ROI investigation within them. However, the existence of tissue often results in ineffectiveness of various image processing techniques like edge detection, rotation and etc., leading to undesired effect on SDROI extraction. In this paper, we successfully remove the tissue by exploiting the characteristics exhibited by the tissue. Experiment on one real data

	.1	.15	.2	.25	.3	.35	.4	.45	.5	.55	.6	.65	.7	.75	.8	.85	.9	.95	1
MSnewborn	4	4	4	4	4	4	3	3	3	3	3	2	2	2	2	2	1	0	0
MS3y	0	0	1	1	1	4	3	3	3	3	3	2	2	2	2	2	1	1	0
MS3y6m	2	2	4	3	3	3	3	3	3	3	3	2	1	1	1	1	0	0	0
MS4y	0	1	4	4	4	4	4	4	3	3	3	3	3	3	2	2	1	1	0
MS4y6m	0	0	0	0	2	2	2	2	1	1	3	3	1	1	0	0	0	0	0
MS5y	0	0	0	0	0	1	4	4	4	4	3	3	3	2	2	2	1	0	0
MS6y	0	0	0	1	2	2	2	4	4	3	2	2	2	2	0	0	0	0	0
MS7y	4	4	4	4	4	4	4	4	3	3	2	2	2	2	2	1	1	0	0
MS8y	0	1	1	3	3	3	2	3	3	3	3	3	3	1	1	1	1	0	0
MS9y	1	1	1	2	4	4	4	3	3	3	3	3	2	1	1	1	0	0	0
MS10y	4	4	4	4	4	4	4	4	4	4	4	3	2	2	2	2	1	0	0
MS11y	0	1	1	1	1	2	2	2	2	2	2	1	1	2	2	2	2	1	0
MS11y6m	2	2	4	4	4	4	4	4	3	2	2	2	2	2	2	1	0	0	0
MS12y6m	1	2	4	3	3	3	3	3	3	3	3	3	3	3	2	1	1	1	0
MS13y	1	1	2	3	3	4	3	3	3	3	3	3	3	3	1	2	1	0	0
MS13y6m	2	2	4	3	3	3	2	2	2	2	2	1	1	1	1	0	0	0	0
MS14y	4	4	4	4	4	4	4	4	4	3	3	3	3	3	3	2	1	1	0
MS15y	2	4	4	4	4	4	4	4	3	3	3	2	2	2	2	2	1	0	0
MS15y6m	1	2	2	4	4	4	4	4	4	4	4	3	3	3	2	2	1	1	0
MS16y	4	4	4	4	4	4	4	3	3	3	3	3	3	3	2	1	1	1	0
MS17y	2	4	4	4	4	4	4	4	3	3	3	3	3	3	3	2	1	1	0
MS18y	2	2	2	4	4	4	4	4	4	4	3	3	3	3	2	2	0	0	0
MS19y	2	4	4	4	4	4	4	4	4	3	3	3	3	2	2	2	0	0	0

Table 1: Experiment result in terms of the number of correctly extracted digits without reducing the tissue influence. The numbers of the first line (from .1 to 1) correspond to different SDROI threshold values, and the labels of the first column (e.g.,15MS6y) correspond to different source hand X-ray images.

	.1	.15	.2	.25	.3	.35	.4	.45	.5	.55	.6	.65	.7	.75	.8	.85	.9	.95	1
1MSnewborn	4	4	4	4	4	4	4	4	4	3	3	3	3	3	3	2	2	1	0
10MS3y	4	4	4	4	4	4	4	2	2	2	2	2	2	2	2	2	2	2	0
11MS3y6m	4	4	4	4	4	3	3	3	3	3	3	3	3	3	3	2	2	1	0
12MS4y	4	4	4	4	4	4	4	4	4	4	3	3	3	3	2	2	2	1	0
13MS4y6m	0	0	0	0	1	1	1	2	1	1	1	2	3	2	2	0	0	0	0
14MS5y	1	2	2	4	4	3	3	3	3	3	3	3	3	2	1	1	1	1	0
15MS6y	2	2	4	4	4	4	4	4	4	4	4	3	3	3	3	3	3	0	0
16MS7y	4	4	4	4	4	4	4	4	4	4	4	3	2	2	2	2	2	1	0
17MS8y	4	4	4	4	4	4	3	3	3	3	3	3	3	3	3	2	2	2	0
18MS9y	4	4	4	4	4	4	4	4	4	4	4	3	3	2	2	2	2	1	0
19MS10y	4	4	4	4	4	4	4	4	4	4	4	4	3	3	2	2	2	1	0
20MS11y	4	4	4	4	4	4	4	4	4	4	3	3	2	2	2	2	2	1	0
21MS11y6m	4	4	4	4	4	4	4	4	4	4	3	3	2	2	2	2	1	1	0
22MS12y6m	4	4	4	4	3	3	3	3	3	3	3	3	3	2	2	2	1	1	0
23MS13y	4	4	4	4	4	4	3	3	3	3	3	3	3	3	2	2	2	1	0
24MS13y6m	4	4	4	3	3	3	3	3	3	3	2	2	2	2	2	1	1	1	0
25MS14y	4	4	4	4	4	4	4	4	3	3	3	3	3	2	2	2	2	2	0
26MS15y	4	4	3	3	3	3	3	3	3	3	3	3	3	3	2	2	1	1	0
27MS15y6m	4	4	4	4	4	4	4	4	4	4	4	4	3	3	2	2	1	1	0
28MS16y	3	3	3	3	3	3	3	3	3	2	2	2	2	2	2	1	1	1	0
29MS17y	4	4	4	4	4	4	4	4	4	4	4	4	4	4	2	2	2	0	0
30MS18y	4	4	4	4	4	4	4	4	4	4	4	2	2	1	1	1	1	1	0
31MS19y	4	4	4	4	4	4	3	3	3	3	3	3	3	3	3	2	2	2	0

Table 2: Experiment result in terms of the number of correctly extracted digits with reducing the tissue influence. The numbers of the first line (from .1 to 1) correspond to different SDROI threshold values, and the labels of the first column (e.g.,15MS6y) correspond to different source hand X-ray images.

	.1	.15	.2	.25	.3	.35	.4	.45	.5	.55	.6	.65	.7	.75	.8	.85	.9	.95	1
Scenario 1	41	53	67	74	79	86	84	85	78	74	72	63	58	53	42	36	17	9	0
Scenario 2	89	90	91	92	92	90	87	86	84	82	77	73	68	62	53	45	40	26	0
Scenario 1'	43	56	70	77	81	88	85	86	81	76	72	63	59	55	44	38	18	9	0
Scenario 2'	93	94	95	97	95	93	90	88	86	84	80	74	68	63	53	47	42	27	0

Table 3: The summary of overall success rate(%). Scenario 1: without tissue reducing, bad case 5 included; Scenario 2: with tissue reducing, bad case 5 included; Scenario 1': without tissue reducing, bad case 5 excluded; Scenario 2': with tissue reducing, bad case 5 excluded. The numbers of the first line (from .1 to 1) correspond to different SDROI threshold values.

set shows its effectiveness. The best result in terms of overall success rate on SDROI extraction, without considering the single bad case 'MS4y6m' where digits overlap too much, reaches 97% v.s. 88% if *not* using tissue removing. Except the digits overlap issue, other factors causing failure of SDROI extraction are also observed like *over-angled posture* and *non-consistency in lengths of digits* for instance. To relief the influence of these factors will be addressed in our future work.

5 Acknowledgement

References

[1] A. F. Roche, C. G. Rohmann, N. Y. French, and G. H. Davila, Effect of training on replicability of assessment of skeletal maturity (Greulich-Pyle), *Amer. J. Roentgenol.*, vol. 108, pp. 511-515, 1970.

[2] A. J. L. Cole, L. Webb, and T. J. Cole, Bone age estimation: A comparison of methods, *Brit. J. Radiol.*, vol. 61, pp. 683-686, 1988.

[3] A. Poznanski, S. M. Garn, J. M. Nagy, and J. C. Gall, Metacarpophalangeal pattern profiles in the evaluation of skeletal malformations, *Radiology*, vol. 104, pp. 1-11, 1972.

[4] D. B. Darling, *Radiography of Infants and Children*, 1st ed. Springfield, IL: Charles C Thomas, 1979, ch. 6, pp. 370-372.

[5] D. Hua and A. Youssef, A Sectrum-based Method for Single Digit Region of Interest (ROI) Extraction, to be submitted.

[6] D. J. Michael and A. C. Nelson, HANDIX: A model-based system for automatic segmentation of bones from digital hand radiographs, *IEEE Trans. Med. Imaging*, vol. 8, pp. 64-69, 1989.

[7] D. R. Kirks, Practical Pediatric Imaging. *Diagnostic Radiology of Infants and Children*, 1st ed. Boston, MA: Little, Brown & Co., 1984, ch. 6, pp. 198-201.

[8] E. Pietka, A. Gertych, S. Pospiech, F. Cao, H. K. Huang, and V. Gilsanz, Computer-Assisted Bone Age Assessment: Image Preprocessing and EpiphysealMetaphyseal ROI Extraction, *IEEE Trans. on Medical Imaging*, Vol, 20, No. 8, August 2001.

[9] E. Pietka, M. F. McNitt-Gray, and H. K. Huang, Computer-assisted phalangeal analysis in skeletal age assessment, *IEEE Trans. Med. Imag.*, vol. 10, pp. 616-620, 1991.

[10] G. R. Miler, R. K. Levick, and R. Kay, Assessment of bone age: A comparison of the Greulich and Pyle and the Tanner and Whitehouse methods, *Clin. Radiol.*, vol. 37, pp. 119-121, 1986.

[11] J. Kosowicz, The Roentgen appearance of the hand and wrist in gonadal dysgenesis, *Radiology*, vol. 93, pp. 354-361, 1965.

[12] J. M. H. Buckler, How to make the most of bone ages, *Archives Disease Childhood*, vol. 58, pp. 761-763, 1983.

[13] J. M. Tanner and R. H. Whitehouse, *Assessment of Skeletal Maturity and Prediction of Adult Height (TW2 Method)*. New York: Academic, 1975.

[14] L. Bocchi, F. Ferrara, I. Nicoletti, and G. Valli, An Artificial Neural Network Architecture for Skeletal Age Assessment, *IEEE International Conference on Image Processing*, September 14-17, 2003.

[15] M. F. McNitt-Gray, E. Pietka, and H. K. Huang, Computer assisted phalangeal analysis in skeletal age assessment, *IEEE Trans. Med. Imag.*, vol. 10, pp. 616-620, 1991.

[16] N. Otsu, A threshold selection method from gray-level histograms, *IEEE Trans. Syst., Man, Cybern.*, vol. SMC-9, pp. 62-66, 1979.

[17] P. Soille, *Morphological Image Analysis: Principles and Applications*, Springer, 1999, pp. 164-165.

[18] S. N. C. Cheng, H. Chan, L. T. Niklason, and R. S. Alder, Automated segmentation of regions on hand radioraphs, *Med. Phys.*, vol. 21, pp.1293-1200, 1994.

[19] S. Wastl and H. Dickhaus, Computerized Classification of Maturity Stages of Hand Bones of Children and Juveniles, *18th Annual International Conference of the IEEE Engineering in Medicine and Biology Society*, Amsterdam 1996 4.5.3: Image Pattern Analysis 1.

[20] T. E. Keats and L. B. Lusted, *Atlas of Roentgenographic measurement*, Year Book Medical Publishers, Chicago, IL, 1985.

[21] T. S. Levitt and M. W. Hedgcock, Model-based analysis of hand radiographs, *Proc. SPIE*, vol. 1093, pp. 563-570, 1989.

[22] W. W. Greulich and S. I. Pyle, *Radiographic Atlas of Skeletal Development of Hand Wrist.* Stanford, CA: Standord University Press, 1971, 2nd, ed.